Fixed Bed Adsorption/Desorption of Valeric Acid from Aqueous Solution Using Granular Activated Charcoal

Yousefi Jolandan Hannaneh; Ashraf Talesh, Seyed Siamak*[+]

Department of Chemical Engineering, Faculty of Engineering, University of Guilan, Rasht, I.R. IRAN

ABSTRACT: *In this research, the capability of Granular Activated Charcoal (GAC) for adsorbing Valeric acid (VA) from an aqueous solution was investigated in a fixed-bed column. The effect of important parameters, such as flow rate, initial concentration, bed depth, and the temperature was considered. The maximum adsorption capacity was achieved equal to 750.93 (mg/g). Length of Mass Transfer Zone (MTZ), Length of Unused Bed (LUB), and Carbon Usage Rate (CUR) were calculated. Three dynamic models (Thomas, B-A, and Yoon-Nelson) were applied in different situations. The Yoon–Nelson and Thomas models were found suitable for predicting the initial part of breakthrough curves. The FTIR tests indicated that the adsorption of VA on GAC has mainly occurred physically. The feasibility of desorbing VA from saturated GAC was also determined. The column was regenerated by using deionized water in three cycles. The desorption percentage of Valeric acid in the second and third cycles were 73% and 35%, respectively.*

KEYWORDS *Breakthrough curve; Dynamic adsorption; Granular activated charcoal; Valeric acid.*

INTRODUCTION

The removal of carboxylic acid from aqueous solution is an important subject for industries due to effects of purification steps on production cost [1]. Furthermore one of the great concerns of societies is how to remove odorous species from water and wastewater [2]. Valeric acid (pentanoic acid) is an alkyl carboxylic acid with a very unpleasant odor [3]. It has origin in the flowering plant valerian [4]. The most important usage of Valeric acid is in the synthesis of its esters [5]. Ethyl valerate and pentyl valerate are considered as food additives because of their fruity flavors [3]. In addition, Valeric acid is used to manufacture of perfumes, synthetic lubricants, agricultural chemicals, and pharmaceuticals as chemical intermediate. It is partly toxic to aquatic organisms higher than the certain limit [6]. Recently, Valeric acid has enticed significant attention as an intermediate in production of cellulosic biofuels [7]. International Program on Chemical Safety (IPCS) has categorized Valeric acid as a harmful factor for the aquatic life [2]. Valeric acid has been found in wastewater from 0.5 g/L up to 25 g/L [8].Some methods such as extraction [9, 10], ultrafiltration [11] and batch adsorption [1, 12, 13] have been proposed for separation of Valeric acid from aqueous solution or fermentation broth. However these treatments demand high costs, complicated equipment, and organic solvents that may be injurious to the environment [14]. Adsorption process has been identified as an efficient method in most of the industrial water and wastewater treatment [15, 16].

* *To whom correspondence should be addressed.*
+ E-mail: s_ashraf@guilan.ac.ir
1021-9986/2021/1/143-156 9/$/5.09

It is one of the most desired separation technics due to its remarkable efficiency, uncomplicated recovery, inexpensive and simple operation [17, 18]. Economically, the batch system is not effective except for a short time, and it needs a large amount of adsorbent. In contrast, the column system is economical and practical. As well as column system can be used under high effluent flow rates [19]. It has been employed in many contamination control methods such as removal of toxic organic composition by activated carbon or removal of ions by an ion-exchange bed [20]. Ion exchange technique has been broadly applied in adsorption process. A few papers have interpreted that ion-exchange resin is a useful adsorbent for organic acid extraction [10, 21-24]. In order to purify gas, water and wastewater, for removal of color, odor and organic pollutants, activated charcoal has been widely used in many processes [2, 25]. It is the most commonly used porous adsorbents due to its high surface and wide range of pore sizes and hydrophobic surfaces [2, 18, 26-28]. Although adsorption of nonelectrolyte and weak acids from aqueous solution on activated charcoal was reported in many papers, removal of Valeric acid was mentioned in a few of them [29]. Batch adsorption of Valeric acid has been investigated by using activated charcoal but there is no information in the literature about dynamic adsorption of Valeric acid. Dynamic adsorption processes is an appropriate procedure under high flow rate for the industrial scale [14]. The adsorption of trinitrotoluene [26], acid dyes [30], phenol [15] and heavy metals [31] onto activated carbon in fixed bed column has been investigated under different operating conditions.

In this research, the performance of activated charcoal in the removal of Valeric acid from wastewater in fixed-bed column was studied, which has not been done already to the best of our knowledge. The effect of flow rate, initial concentration, bed depth and temperature on breakthrough curve and adsorption-desorption process were investigated. The capability of bed regeneration was examined in three cycles by using deionized water. Three mathematical models (Thomas, Bohart-Adams, and Yoon-Nelson) were applied to anticipate the breakthrough curves.

Material

Granular of Activated charcoal (CAS Number: 7440-44-0, diameter of 1.5 mm, molar mass 12.0 1 g/mol, melting point 3550 ^{0}C, bulk density 44 kg/m^3) and Valeric acid (pentanoic acid) were purchased from Merck (Germany). Valeric acid with an assay of 98% and molecular mass of M_w=102.13 was dissolved in deionized water to prepare Valeric acid solutions.

EXPERIMENTAL SECTION

Procedure

The inner diameter of dynamic column, the height of column and the bed depth were selected in the range of 1.5-2, 30-50 and 5-15 Cm, respectively, in the literatures [32-37]. In this research, for appropriate selecting of the column feature criteria, two columns with 1.5 and 50 cm, and another one with 1.7 and 35 cm, height and inner diameter had tested, respectively. Although the first one had the high residence time, the accessibility to the adsorbent was difficult and the inappropriate distribution of adsorbent leads to channeling. So, after initial analysis for evaluation of the performance of the designed columns the performance efficiency of the former was found acceptable and was selected for the column feature of this research. The experimental setup Fig. 1, was composed of a double-glazed glass column (35 cm height and 1.7 cm inner diameter), a feed tank and a digital peristaltic pump (Zistco model P466). Activated charcoal was set inside the column at different bed depths (7, 9, 11 and 13 cm). Then the column was washed with deionized water to remove impurities and air bubbles. The solution was pumped at different flow rates (3, 5 and 8 mL/min) into the fixed bed column. Different concentrations (3, 10, 20 g/L) of Valeric acid solution were chosen as initial concentration of feed. In order to investigate the effect of temperature, three levels of temperatures (303, 313 and 323 K) were chosen. Every five minutes, samples were taken from the bottom of the column. The concentration of Valeric acid in the samples was determined using an UV-Vis spectrophotometer (Varian Cary 50 UV-Vis Spectrophotometer) with detecting wavelength at 237 nm.

Dynamic adsorption studies

Mathematical description of dynamic adsorption

Effluent concentration to initial concentration (C/C0) is a function of time. The total adsorbed Valeric acid in the bed was estimated as follows [38]:

$$q_{total} = \frac{Q\,A}{1000} = \frac{Q}{1000}\int_0^{t_{total}} C_{ad}\,dt = \frac{Q}{1000}\int_0^{t_{total}} (C_0 - C_e)\,dt \quad (1)$$

The equilibrium capacity of the bed was acquired by using below equation [38]:

$$q_{eq} = \frac{q_{total}}{X} \quad (2)$$

The total amount of Valeric acid which entered to the bed, was determined using the following equation [38]:

$$m_{total} = \frac{C_0 Q t_{total}}{1000} \quad (3)$$

$$\text{Total Removal\%} = \frac{q_{total}}{m_{total}} \times 100 \quad (4)$$

The Empty Bed Contact Time (EBCT) in the column is the time necessary for the liquid for filling the empty column, is calculated as follows [38].

$$EBCT = \frac{V_C}{Q} = \frac{H}{\vartheta} \quad (5)$$

The value of EBCT effects on the breakthrough time and the shape of breakthrough curve. Higher EBCT leads to higher contact time. So the concentration of outlet solution decreases in higher EBCT [38].

The number of bed volumes treated before breakthrough can be calculated by Eq.6 [39].

$$BV = \frac{\text{volume of water treated at breakthrough point (l)}}{\text{volume of adsorbent bed (l)}} \quad (6)$$

The adsorbent exhaustion rate (AER) was obtained from Eq.7 for the breakthrough of 1% [38]

$$AER = \frac{\text{mass of adsorbent in column (g)}}{\text{through put volume at breakthrough (l)}} \quad (7)$$

The Adsorbent exhaustion rate is used to determine the regularity which can be applied to substitute the adsorbent [38].

Mass transfer zone and breakthrough curve

The MTZ is the part of the bed where the main adsorption is taking place. The exchange rate between phases and the adsorbent‘s removal efficiency are determined by MTZ. Faster exchange causes smaller heights of MTZ, so the numbers of transfer unite expand. Increasing the flow rate or the initial concentration of acid leads to the competition among acid molecules for choosing an adsorption site. For rectifying this situation, the MTZ develops its height and suggests more sites to the Valeric acid molecules. As a result the adsorption kinetic is improved by increasing the bed depth [40]. The height of MTZ is controlled by flow rate, initial concentration, temperature and so forth. The data are estimated between the bed capacity T_V at breakthrough point and T_C, the total bed capacity [38].

$$T_V = \int_0^{T_b} \left(1 - \frac{c}{c_0}\right) dt \quad (8)$$

$$T_c = \int_0^{\infty} \left(1 - \frac{c}{c_0}\right) dt \quad (9)$$

$$MTZ = \left(1 - \frac{T_V}{T_C}\right) H \quad (10)$$

Breakthrough at 1% and exhaustion at 95% have been assumed, so that the Rate of the Mass Transfer Zone (RMTZ) movement is achieved by Eq. (11)

$$RMTZ = \frac{MTZ}{t_{0.95} - t_{0.01}} \quad (11)$$

Length of unused bed (LUB)

In continuous setup, at first seconds, the most mass transfer occurs near the entrance of the bed and the rest of the length bed remains unused. During the experiments the length of MTZ is increased, so LUB is decreased. LUB is defined as follows[41]:

$$LUB = H\left(1 - \frac{W_b}{W_{sat}}\right) \quad (12)$$

$$W_b = \frac{F_A \int_0^{t_b} \left(1 - \frac{c}{c_0}\right) dt}{H \times \rho_b} \quad (13)$$

$$W_{sat} = \frac{F_A \int_0^{t^*} \left(1 - \frac{c}{c_0}\right) dt}{H \times \rho_b} \quad (14)$$

$$t^* = \frac{H \rho_b (w_{sat} - w_0)}{u_0 c_0} \quad (15)$$

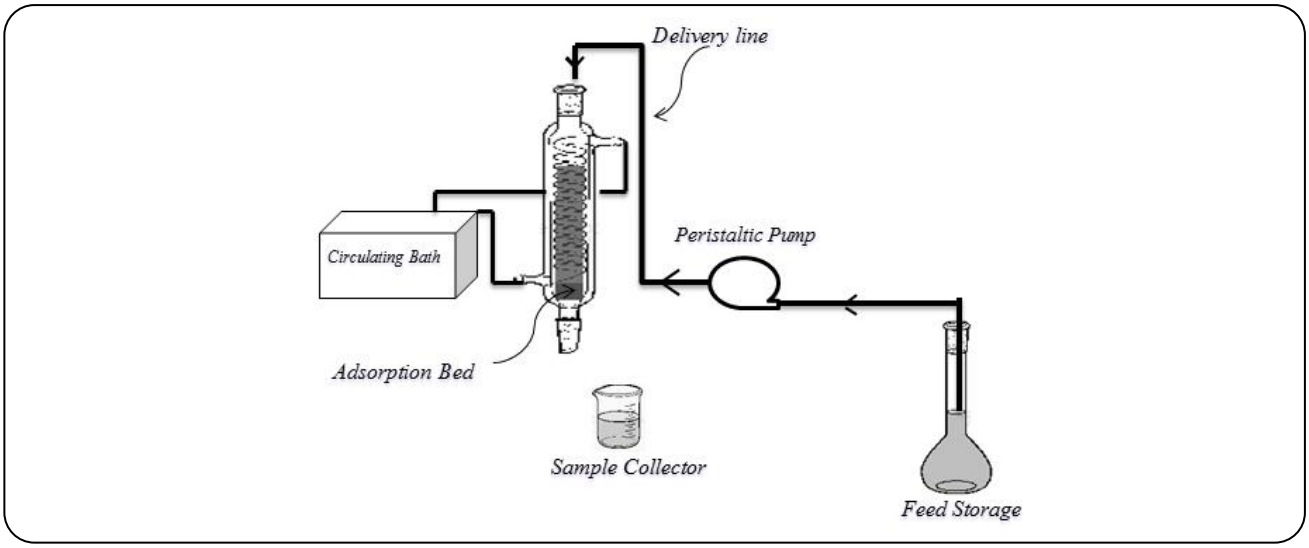

Fig. 1: Experimental set up for the fixed-bed adsorption process.

Carbon Usage Rate (CUR)

The control of the exhausted carbon is largely affected by the CUR based on the cost-effectiveness [42]. The rate of carbon exhaustion and carbon replacement/regeneration frequency is determined by CUR. The longer contact time takes the more carbon effectiveness improves. The percentage of exhausted carbon at breakthrough is increased by deeper beds. The CUR shows the amount of GAC which is needed for a unit volume of water purification. CUR can be determined as follow [43, 44]:

$$CUR = \frac{M}{V} = \frac{\rho_{CAC}}{V'} \quad (16)$$

$$V' = \frac{V_b}{V_c} \quad (17)$$

$$CUR = \frac{EBCT}{t_b} \quad (18)$$

RESULT AND DISCUSSION

The effect of adsorbent type

At many contamination control methods, activated carbon and ion-exchange resins have been used as adsorbents [20]. In this research, for comparison, the ability of Amberlysite A26 (OH) and Amberlite in the removal of Valeric acid from aqueous solution was also investigated. According to Fig. 2, sharper breakthrough curve, shorter breakthrough and exhausted time are obtained using resins as an adsorbent. Also it is clear that activated charcoal exhibited sufficient capacity to removal of Valeric acid in compared with the resins [45]. The activated charcoal showed the best performance (the highest removal percent and equilibrium capacity and the most breakthrough time in the same situation). Besides, activated charcoal is the more available and low cost adsorbents compared with resins. The interaction between Valeric acid and active phase of granular activated charcoal is small, so the regeneration is easier than ion-exchange resins. Moreover, Activated carbons can be used at high temperature [46, 47].

FT-IR analysis

The FTIR spectrum of GAC before adsorption, after one and three time adsorption has been shown in Fig. 3. The large peak around 3446 (cm^{-1}), is related to the stretching vibration of H-bonded hydroxyl groups and chemisorbed water. A sharp peak at 1639 (cm^{-1}) and a medium at 667 (cm^{-1}) are attributed to stretching vibration of carbon double bond and carbon chloride (C-CL), respectively. The peak at 1385 (cm^{-1}) and 2361 (cm^{-1}) could be due to bending and stretching vibration of $–CH_3$, and a very weak peak at 2073 (cm^{-1}) is proved the presence of C≡C in AC. The only difference which is observed is a peak at 1550 (cm^{-1}) which is sharper than before of adsorption. This small shift indicates that the adsorption of Valeric acid on activated charcoal is mainly occurred physically [48-50].

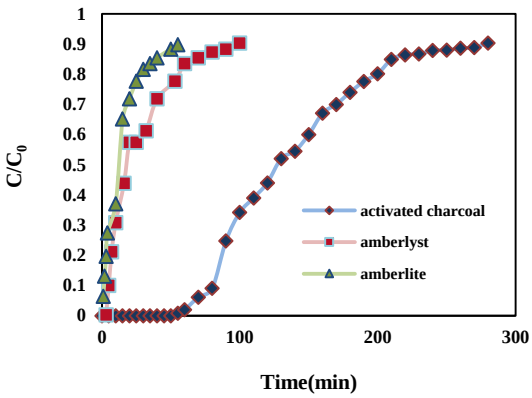

Fig. 2: Effect of adsorbent type on breakthrough curve (H=11 Cm, C_0=10 gr/lit, Q=5 ml/min).

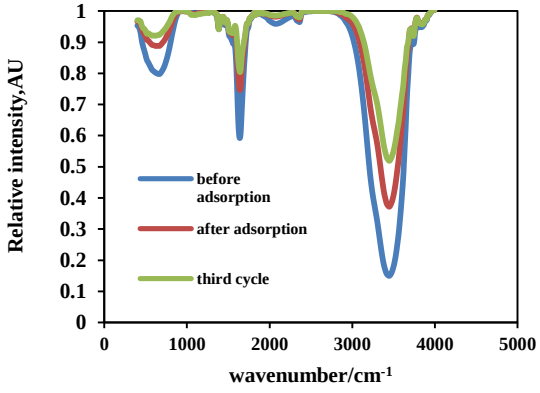

Fig. 3: FT-IR spectrum of GAC before adsorption, after adsorption and after three time adsorption.

The effect of bed depth on breakthrough curve

In order to analyze the influence of the bed height, flow rate and concentration were fixed in 5ml/min and 10 g/L respectively, and the height was changed among the different levels as 7, 9, 11 and 13. According to Fig. 4, when the bed depth increases, breakthrough time, the maximum capacity of column and removal percentage increases as well. In fact, when the bed depth increases, the adsorption sites and the contact time between solution and adsorbent are enhanced. Accordingly, higher bed depth saturates slower and breakthrough time decreases. The exhaustion time of the adsorbent is delayed in higher bed depth [38]. The axial dispersion is predominant mechanism in the adsorbate transfer for the shorter bed [33]. The porosity distribution which is the main properties of the pack was affected by the packing procedure. Therefore, this procedure shifts the flow pattern and fluid distribution inside the pack [51]. In higher bed depth which is more than 11(Cm), adsorbent is accumulated in some part of the bed, so channeling is occurred. In fact inappropriate distribution of adsorbent and channeling phenomena reduces the removal percentage for 13(cm) bed depth. As a result, the optimum bed depth is obtained 11(cm). As the bed depth increases, the calculated value of AER decreases, but the BV number increases. The computed CUR (Table 2) exhibits that the higher bed depth reduces the amounts of required GAC for a unite volume of contaminated water.

The effect of initial concentration on the breakthrough curve

The solution with different concentration (3, 10, 20 cm) was passed through the column (11 cm depth) at flow rate of 5(mL/ min) to show the influence of initial concentration on breakthrough times. As shown in Fig. 5, when the initial concentration increases, sharper breakthrough curve is obtained. In fact, higher concentration causes higher concentration gradient. Therefore, driving force for mass transfer increases, and the bed saturates faster [33]. The values of CUR and AER are increased with increasing the initial concentration, whereas the number of BV is decreased (Tables 1 and 2). At low concentration of Valeric acid (3gr/lit), surface chemistry is the predominate factor for adsorption. In fact, an increase in water molecules leads to competition between Valeric acid and water for the active sites on the surface. So the interactions of surface groups with water affect the process of Valeric acid adsorption. Besides, Valeric acid molecules occupy more area when adsorbed to the surface with its hydrocarbon chain parallel compared to the situation adsorbed perpendicular to the surface [2]. Therefore, these various behavior leads to different trend of the curve with the concentration of 3g/L. On the other hand, the driving force is the conquering factor at high concentrations (10 and 20gr/lit). As the driving force for mass transfer increases, the bed saturates faster and the sharper breakthrough curve is obtained. In fact, at higher concentrations (10 and 20 gr/lit) more Valeric acid molecules are available for interacting *via* adsorbents, the water molecules find less area of adsorbent surface for interaction and cannot disorder normal procedure of adsorbents, so the same trend are exhibited for concentration curve of 10 and 20 g/L.

Table 1: Summary of the fixed bed parameters at breakthrough and exhaustion points for VA adsorption onto GAC.

H(Cm)	Q(ml/min)	C_0(g/lit)	T(k)	q_e (mg/g)	R%	BV	AER(g/l)
11	5	3	30	336.92	45.96	23.63	0.021
11	5	10	30	734.32	35.01	16.42	0.037
11	5	20	30	416.36	35.56	3.21	0.103
11	3	10	30	655.61	42.76	12.49	0.037
11	8	10	30	413.82	22.09	4.81	0.117
7	5	10	30	158.78	18.08	1.89	0.436
9	5	10	30	384.03	28.38	5.14	0.093
13	5	10	30	750.93	32.56	15.25	0.038
11	5	10	40	561.72	34.37	9.61	0.051
11	5	10	50	427.23	35.03	7.71	0.079

Table2. Carbon usage rate (CUR), length of mass transfer zone (MTZ) and length of unused bed (LUB) at different column conditions for Table

H (Cm)	Q (mL/min)	C0 (g/L)	T (K)	EBCT (min)	CUR_{bp} (g/L)	CUR_e (g/L)	MTZ (Cm)	RMTZ (Cm/min)	Lub (Cm)
11	5	3	303	4.994	19.51	5.858	6.079	0.022	4.799
11	5	10	303	4.994	28.076	7.194	6.865	0.028	5.196
11	5	20	303	4.994	143.89	24.234	7.696	0.097	6.934
11	3	10	303	8.323	36.89	9.592	6.084	0.020	5.219
11	8	10	303	3.121	95.926	8.993	7.673	0.052	7.939
7	5	10	303	3.178	244.17	14.363	6.668	0.069	5.706
9	5	10	303	4.086	89.697	10.464	6.382	0.037	5.997
13	5	10	303	5.902	30.231	6.114	8.467	0.023	6.67
11	5	10	313	4.994	47.963	8.688	6.967	0.032	6.335
11	5	10	323	4.994	59.798	12.117	7.591	0.05	6.061

The effect of flow rate on breakthrough curve

As can be seen in Fig. 6, breakthrough generally occurs faster with higher flow rate. As the flow rate increases, the amount of Valeric acid adsorbed onto the bed increases, so it leads to faster saturation. In the other words, at a low flow rate, solution has more time to contact with adsorbent. At a lower flow rate, there is sufficient time for diffusion of Valeric acid molecules into the inner pores of activated charcoal through intraparticle diffusion. As a result, more Valeric acid molecules can be captured by the adsorption sites inside the adsorbent [33]. Based on Tables 1 and 2,) in higher flow rate the values of AER and CUR are increased and the numbers of BV are decreased. Also the maximum value of EBCT is obtained at the lowest flow rate (3ml/min) and the removal percent of Valeric acid decreases with increasing flow rate.

The effect of temperature on breakthrough curve

The effect of temperature on breakthrough curve is shown in Fig. 7. The considered temperatures are 303, 313 and 323 K. The flow rate, initial concentration and bed depth were kept constant at 5 mL/min, 10 g/L and 11 cm, respectively. When the initial temperature increases, the breakthrough time, the exhaustion time, and adsorption capacity decrease. Nevertheless, the removal percentage almost is constant (Table 1). In fact the breakthrough time

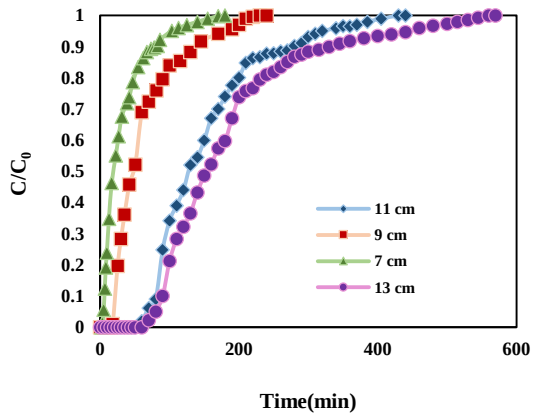

Fig. 4: The effect of bed depth on breakthrough curve (C0=10 gr/lit, Q= 5 ml/min and T=303 k).

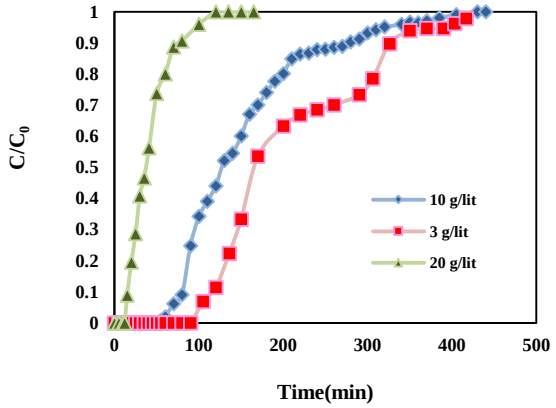

Fig. 5: The effect of initial concentration on the breakthrough curve (H=11 Cm, Q= 5 gr/lit and T= 303 K).

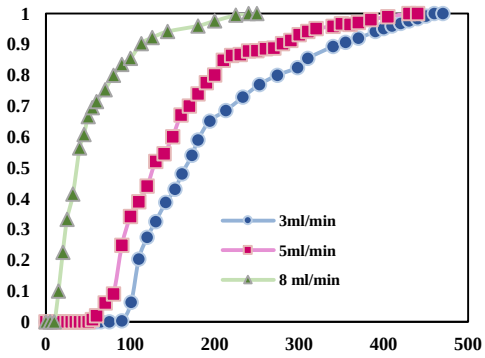

Fig. 6: The effect of flow rate on breakthrough curve (H=11 Cm, C0= 5 gr/lit, T=303 K).

decreases because the adsorption is an exothermic process, increasing the temperature has an inverse effect on the efficiency of the process. Generally, physical adsorption is an exothermic process because it is accompanied by a reduction in free energy and entropy of the adsorption system [52].As the temperature increases, the amounts of CUR and AER (Tables 1and 2) increase too. In other word, a reverse relationship is determined between temperature and BV number [53].

Desorption and column regeneration

One of the environmental problems is the exhausted adsorbent which contains hazardous material[54]. Moreover replacing the saturated bed imposes the high cost. The demand of new adsorbent and disposal of exhausted adsorbent is reduced by regeneration of the bed [40].

The bed regeneration in physical adsorption is more convenient than chemical adsorption [55]. According to the FTIR analysis (Fig. 1), the adsorption of Valeric acid by activated charcoal is mainly occurred physically, so the regeneration is suitable for this process.

Usually in dynamic adsorption, some parts of column remain unused [38]. Therefore, reusing is really important. Adsorption- desorption was done in three steps in fixed-bed column. Desorption process was done by pumping deionized water to the saturated bed. When the adsorption cycles are increased, the breakthrough curves shift to the left. Therefore, the breakthrough time and exhaustion time are reduced. The values of desorption is evaluated by using Eq.19.

$$\text{Desorption} = \frac{q_d}{q_{total}} \qquad (19)$$

As can be observed from Table 3, in the second and third cycle, desorption percentage is reduced to 71.15% and 35.46%, respectively. It is found that in the consecutive cycle, the desorption percentage and adsorption capacity are reduced because of the absorbent was used nonstop and deteriorated. Furthermore, changes in the flow and mass transfer conditions within the column can cause this anomaly and it is expected that there is still some amount of adsorbed Valeric acid on the adsorbent surface [38]. Consequently, it is possible to regenerate the column using deionized water because of high performance and low price of it. According to the FT-IR analysis (Fig. 3), the adsorption of Valeric acid

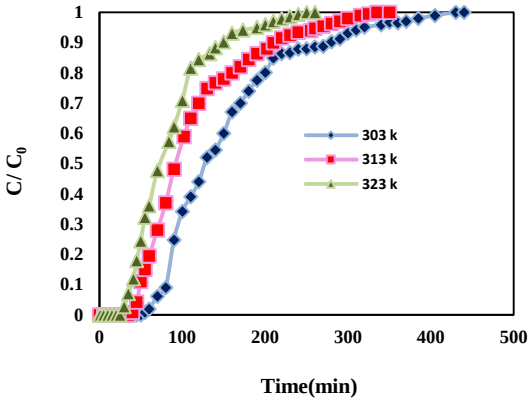

Fig. 7: The effect of temperature on breakthrough curve (H=11 Cm, C_0=10 g/lit and Q=5 mL/min).

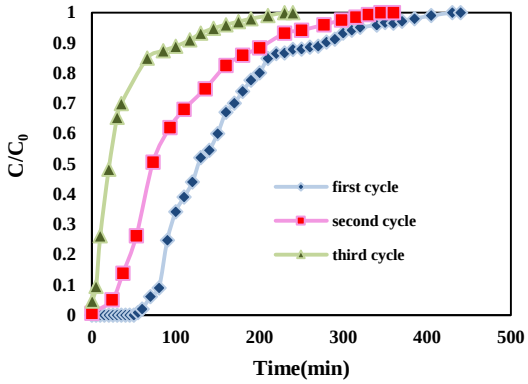

Fig. 8: Breakthrough curves for adsorption of VA onto GAC during regeneration cycles.

The effect of bed depth on breakthrough curve

by activated charcoal is mainly occurred physically, so the regeneration is suitable for this process. As can be observed from Table 3, in the second and third cycle, desorption percentage is reduced to 71.15% and 35.46%, respectively. It is found that in the consecutive cycle, the desorption percentage and adsorption capacity are reduced. The scrutiny of the FT-IR analysis of GAC after adsorption Show the appearance of a weak peak at 1550 (cm^{-1}) which is related to formation of chemical bonds with amid II of carboxylic group (RCONHR) [56]. This peak stayed fixed after desorption and the generation process did not effect on it. A medium peak at 667 (cm^{-1}) is attributed to stretching vibration of carbon double bond and carbon chloride (C-CL), where this peak shifted to the lower frequency after each cycle, because the absorbent was used frequent. So these two alteration act as barriers for desorption process to occur completely. the desorption of Valeric acid failed to done completely in each cycle and the adsorption of Valeric acid onto activated charcoal was reduced as the regeneration cycle preceded Fig. 8. However, the desorption of Valeric acid failed to done completely in each cycle and the adsorption of Valeric acid onto activated charcoal was reduced as the regeneration cycle preceded. In fact, Alteration of adsorbent structure and the formation of chemical bonds between adsorbate and adsorbents lead to reduction of the desorption percentage [49-50].

Mass transfer zone

As it is shown in Table 2, the length of MTZ is increased with increasing flow rate, bed depth, initial concentration and temperature. The adsorption sites are saturated faster with increasing the initial concentration and the residence time of molecule in bed is reduced with an increase in flow rate. As a result, the rate of mass transfer zone movement increases. For amending this deficiency, the mass transfer zone expands its height and prepares more adsorption sites. The motion of molecules is added in higher temperature hence the rate of MTZ movement increases. Higher bed depth added the adsorption sites so the kinetic of adsorption is increased [55].

Length of unused bed (LUB)

Although in higher bed depth, bigger fraction of bed is used, the optimum amount of LUB is obtained at the bed with 11 Cm height. In fact the best adsorbent distribution inside the column is occurred at this height, so the solution has the best contact with adsorbent and the length of unused bed is decreased. It is shown in Table 2 that when the flow rate increases, the amount of LUB increases too. High flow rate has less time to contact with adsorbent. Therefore, the bigger fraction of bed is unused. The amount of LUB is increased with increasing initial concentration (Table 2). In fact higher concentration causes higher driving force for mass transfer. At the first seconds, the bed is fresh and the entrance of the bed has more capacity for adsorption. Consequently, higher driving force leads to the best mass transfer at this part and the bigger fraction of bed is remained unused. Comparing the amounts of LUB in two different temperatures (303, and 313 K) is shown (Table 2) that with increasing

Table 3: Summary of fixed-bed parameters for adsorption- desorption cycles.

number	q_{eq} (mg/g)	w_{total} (mg)	R%	D%	BV	AER (g/L)	CUR_{bp} (g/L)	CUR_e (g/L)
First	734.318	21500	35.008	-	16.419	0.037	28.076	7.194
Second	522.462	17250	31.045	71.149	6.408	0.171	71.944	8.855
third	185.302	11500	16.516	35.467	1.101	41.12	418.588	15.661

Table 4: Comparsion the result of this study with the previous studies.

method	adsorbents	Maximum adsorption capacity
Batch	Activated carbon BPL from Calgon (bituminous coal origin)	200 mg of acid/g of carbon
Batch	Activated carbon BAX from Westvaco (BAX-1500, wood origin, chemical activation with phosphoric acid	500 mg of acid/g of carbon
DYNAMIC	Granular activated charcoal	750 mg of acid/g of carbon

temperature the amount of LUB is increased. In fact at the higher temperatures, due to the exothermic nature of this process, the bigger part of the bed is unused [19].

The effectiveness of Dynamic adsorption

As it is shown in (Table 4) the effectiveness of previous study for removing Valeric acid by means of activated carbon in batch system was compared with this work. In the previous literature, the effect of pore size was investigated and the maximum adsorption capacity was achieved to 500 mg of acid/g of carbon [2]. In the present work, the dynamic system improved the adsorption capacity up to 750 mg of acid/g of carbon.

MODELING OF BREAKTHROUGH CURVE

In this research, although the dynamic models (B-A, Thomas, Yoon-Nelson and etc.), are not able to predict all parts of the breakthrough, they can predict the primary part of the breakthrough thoroughly. Therefore, these models are considered to be able to describe the initial part of breakthrough curve.

Thomas Model

One of the most common methods for describing the function of adsorption process in fixed bed columns is Thomas Model [57, 58]. Thomas model was improved by excluding external and internal diffusion [31]. This model is attained by the assumption of plug flow and the neglect of axial dispersion in bed column and follows langmuir adsorption-desorption kinetic. The linearized form of Thomas model is presented by Eq. (20) [59, 60].

$$\ln\left(\frac{c_F}{c}-1\right)=\frac{K_{Th}q_F m}{Q}-K_{Th}C_F t \quad (20)$$

Where K_{Th} is the Thomas model constant (ml/min mg), q_0 is the adsorption capacity (mg/g) and m is the mass of adsorbent (g). The amount of k_{Th} is decreased with increasing depth, initial concentration, flow rate and temperature [53]. As it is presented in Table 5, the amount of q_0 is approximated to the experimental adsorption capacity. So the external and internal diffusion aren't limiting steps.

Yoon-Nelson

The Yoon–Nelson model is established on the supposition that the decrease in the probability of adsorption for each adsorbate molecule is proportional to the probability of its adsorption and breakthrough on the adsorbent [32, 61]. The linearized Yoon–Nelson model for a single component system can be represented by Eq. (21):

$$\ln\left(\frac{C_t}{C_0-C_t}\right)=K_{YN}(t)-K_{YN}\tau \quad (21)$$

Where K_{YN} is the rate constant (min^{-1}) and τ is the time required for 50% breakthrough [61]. It should be noted that the increase in the flow rate, bed depth, and temperature decreases the K_{YN}. Further, an inverse relationship is obtained between initial concentration and K_{YN} [59]. In addition, the calculated τ values are almost near to experimental times obtained for 50% breakthrough (Table 6).

Table 5: Thomas model parameters at different experimental conditions.

	RMSE	K_{Th}	q_0	q_{exp}
7 Cm	0.03613	0.04919	85.3506	89.97
9 Cm	0.404	0.03681	67.1023	183
11 Cm	0.0073	0.0099	491.54	466.553
13 Cm	0.2895	0.00813	479.249	431.035
3 gr/lit	0.0088	0.01483	241.339	223.89
20 gr/lit	0.0427	0.0071	300.974	232.09
3 ml/min	0.0514	0.02225	335.78	346.64
8 ml/min	0.0369	0.01911	205.01	175.43
313 K	0.1022	0.01639	321.356	332.53
323 K	0.0482	0.01193	283.516	263.78

Bohart-Adams model (B-A)

Bohart and Adams presented a model on the basis of surface reaction theory. This equation is resulted by assumption of non-instantaneous adsorption equilibrium.

$$\ln\left(\frac{c}{c_0}\right) = k_{BA} c_0 t - k_{BA} N_0 \frac{Z}{F} \qquad (22)$$

Where k_{BA} is the kinetic constant (L/mg min), N_0 is the saturation concentration (g/L) and F is the superficial velocity (cm/min) defined as the ratio of the volumetric flow rate Q (cm^3/min) to the cross-sectional area of the bed (cm^2) [39, 59, 60]. It is found (Table 7) that a direct relationship exists among bed depth, flow rate, initial concentration, temperature and k_{BA}. However, the value of N_0, is increased with increasing bed depth, initial concentration and decreasing the flow rate and temperature.

CONCLUSIONS

In the present study, a thorough laboratory investigation was carried out for evaluating a fixed bed column performance to removal Valeric acid from wastewater. Activated charcoal as adsorbent for removing Valeric acid from aqueous solution was proved efficiency. Flow rate, bed depth, initial concentration and temperature were investigated. The adsorption capacity and removal percentage was increased with an increase in bed depth and reducing initial concentration and flow rate. The variation of temperature showed that the adsorption of Valeric acid on activated charcoal was an exothermic process. The adsorption-desorption process was done to evaluate the competence of adsorbent by using deionized water in three cycles. The FTIR analysis, exothermic nature of process, and desorption percentage indicated that the adsorption of Valeric acid on activated charcoal was mainly occurred physically. Three mathematical models (Thomas, B-A, and Yoon-Nelson) were used to obtain the validation of experimental data. The B-A model was found the best model to predict the primary part of breakthrough. The values of AER, CUR and BV were estimated in various conditions. The effect of initial concentration, bed depth, flow rate, and temperature on MTZ and LUB were determined. All in all, this study evidenced that the activated charcoal is a good candidate for adsorption of Valeric acid from aqueous solution in dynamic process.

Nomenclature

C	Valeric acid concentration at differential time(dt), g/L
C_0	Initial concentration of Valeric acid, g/L
C/C_0	Normalized concentration
C_{ad}	Adsorbed Valeric acid concentration, g/L
F_A	Feed rate of adsorbate per unit cross-sectional area of bed, g/cm^2 min
H	Height of bed, cm
M	Molecular weight, g/mol
M_{total}	The total amount of Valeric acid which entered the bed, mg
Q	Volumetric flow rate, mL/min
q_{eq}	Column maximum capacity, mg/g
q_{total}	Total capacity of the bed, mg
t	Time, min

Table 6: Yoon-Nelson model parameters at different experimental conditions.

	RMSE	K_{YN} (min^{-1})	T	τ_{exp} (min)
7 Cm	0.0345	0.4919	11.164	18
9 Cm	0	0.3164	31.649	48
11 Cm	0.005	0.099	101.061	127
13 Cm	0.0025	0.0813	116.458	153
3 gr/lit	0.0049	0.0445	165.398	166
20 gr/lit	0.0369	0.142	30.940	37
3 ml/min	0.0341	0.2225	115.061	164
8 ml/min	0.0275	0.1911	26.344	37
313 K	0.0558	0.1327	70.582	92
323K	0.0351	0.1193	58.291	74

Table 7: Bohart-Adams model parameters at different experimental conditions.

	RMSE	K_{BA}	N0
7 Cm	0.0481	0.045	0.037
9 Cm	0.071	0.0289	0.058
11 Cm	0.0074	0.00918	0.184
13 Cm	0.0029	0.00743	0.227
3 gr/lit	0.0092	0.012833	0.131
20 gr/lit	0.0446	0.005875	0.287
3 ml/min	0.0556	0.0211	0.080
8 ml/min	0.0367	0.016	0.106
313 K	0.0815	0.0122	0.138
323K	0.0513	0.0107	0.158

t_e Exhausted time, min
t_b Breakthrough time, min
T_c Total bed capacity, mg/g
T_v Bed capacity at breakpoint, mg/g
u_0 Superficial Velocity of fluid, Cm/min
V_b Effluent volume at breakthrough point, mL
V_c Volume of column bed, Cm^3
W_b Concentration on the solid in breakthrough point
W_{sat} Concentration on the solid in saturation point
X Unit mass of adsorbent packed in the column, g
ρ_b Bulk density of bed, kg/ m^3
ν Linear flow rate, Cm/min

Received : Jul. 19, 2019 ; Accepted :Now. 18, 2019

REFERENCES

[1] Gok A., Gok M. K., Asci Y. S., Lalikoglu M., Equilibrium, Kinetics and Thermodynamic Studies for Separation of Malic Acid on Layered Double Hydroxide (LDH), *Fluid Phase Equilibria*, **372** :15-20(2014).

[2] El-Sayed Y., Bandosz T.J., Adsorption of Valeric Acid from Aqueous Solution onto Activated Carbons: Role of Surface Basic Sites, *Journal of Colloid and Interface Science*, **273**: 64-72 (2004).

[3] Schaechter M., "Encyclopedia of Microbiology", Academic Press, Elsevier Science, San Diego, USA, (2009).

[4] Schwab M., "Encyclopedia of Cancer", Springer Science & Business Media, New York City, USA (2008).

[5] Large J. P., Price R., Ayoub P. M., Louis J., Petrus L., Clarke L. , Gosselink H., Valeric Biofuels: a Platform of Cellulosic Transportation Fuels, *Angewandte Chemie International Edition*, **49**: 4479-4483(2010).

[6] A P., Studies on the Molecular Interactions in the Mixture of Antifungal, Pharmaceutical Intermediate and Disinfectant Through Dielectric Parameters, *European Journal of Biomedical and Pharmaceutical Sciences*: 240-245 (2016).

[7] Reyhanitash E., Kersten S. R. A., Schuur B., Recovery of Volatile Fatty Acids from Fermented Wastewater byAdsorptionEhsan Reyhanitash, *ACS Sustainable Chem. Eng*., 9176−9184(2017).

[8] Rodriguez M., Luque S., Luque S., Alvarez J. R., Prados J. C., A Comparative Study of Reverse Osmosis and Freeze Concentration for the Removal of Valeric Acid from Wastewaters, *Desalination* **127**: 1-11 (2000).

[9] Megias-Alguacil D., Tervoort E., Cattin C., Gauckler L.J., Contact Angle and Adsorption Behavior of Carboxylic Acids on α-Al_2O_3 Surfaces, *Journal of Colloid and Interface Science*, **353**: 512-518 (2010).

[10] Uslu H., Adsorption Equilibria of Formic Acid by Weakly Basic Adsorbent Amberlite IRA-67: Equilibrium, Kinetics, Thermodynamics, *Chemical Engineering Journal*,**155**: 320-325(2009).

[11] Senol A., Extraction Equilibria of Valeric Acid Using (Alamine 336/diluent) and Conventional Solvent Systems. Modeling Considerations, *Chemical Engineering and Processing: Process Intensification*, **41**: 681-692(2002).

[12] RodrIuez M., Luque S., Alvarez J.R., Coca J., Extractive Ultrafiltration for the Removal of Valeric Acid, *Jornal of Membrane Science*, **120**: 35-43(1996).

[13] Senol A., Optimization of Liquid-Liquid Equilibria of the Type 2 Ternary Systems (Water+ Valeric Acid+ Aromatic Solvent): Modeling Through SERLAS, *Fluid Phase Equilibria*, **415**: 110-124(2016).

[14] Gao Q., Pan C., Liu F., Lu F., Wang D., Zhang J., Zhu Y., Adsorption Characteristics of Malic Acid from Aqueous Solutions by Weakly Basic Ion-Exchange Chromatography, *Journal of Chromatography A*, **1251**:148-153(2012).

[15] Goshadrou A., A. Moheb, Continuous Fixed Bed Adsorption of CI Acid Blue 92 by Exfoliated Graphite: an Experimental and Modeling Study, *Desalination*, **269** :170-176 (2011).

[16] Başar A., Canan, A Mathematical Model for Adsorption of Surfactant onto Powdered Activated Carbon, *Iran. J. Chem. Chem. Eng. (IJCCE)*, **37(6)**: 125-131(2018).

[17] Davarnejad R., Karimi Dastnayi Z., Cd (II) Removal from Aqueous Solutions by Adsorption on Henna and Henna with Chitosan Microparticles Using Response Surface Methodology, *Iran. J. Chem. Chem. Eng. (IJCCE)*, **38(3)**: 267-281(2019).

[18] Seydoun Ba., et al., Activated Carbon from Olive Wastes as an Adsorbent for Chromium Ions Removal, *Iran. J. Chem. Chem. Eng. (IJCCE)*, **37(6)**: 107-123 (2018).

[19] Karunarathne H., Amarasinghe B., Fixed Bed Adsorption Column Studies for the Removal of Aqueous Phenol from Activated Carbon Prepared from Sugarcane Bagasse, *Energy Procedia*, **34**: 83-90 (2013).

[20] Unuabonah E., Olu-Owolabi B., Fasuyi E., Adebowale K., Modeling of Fixed-Bed Column Studies for the Adsorption of Cadmium Onto Novel Polymer–Clay Composite Adsorbent, *Journal of Hazardous Materials*,**179**: 415-423 (2010).

[21] Gao Q., Liu F., Zhang T., Zhang J., Jia S., Yu C., Jiang K., Gao N., The Role of Lactic Acid Adsorption By Ion Exchange Chromatography, *PloS one*, **5**: e13948 (2010).

[22] Bayazit S.a.S., I.s. Inci, Uslu H., Adsorption of Glutaric Acid and Glyoxylic Acid onto Weakly Basic Ion-Exchange Resin: Equilibrium and Kinetics, *Journal of Chemical & Engineering Data*, **55**: 679-684 (2009).

[23] Bayazit S.a.S., İ. İnci, Uslu H., Adsorption of Lactic Acid from Model Fermentation Broth onto Activated Carbon and Amberlite IRA-67, *Journal of Chemical & Engineering Data*, **56**: 1751-1754(2011).

[24] Natale F. D., Erto A., Lancia A., Musmarra D., Equilibrium and Dynamic Study on Hexavalent Chromium Adsorption onto Activated Carbon, *Journal of hazardous materials*, **281**: 47-55 (2011).

[25] RodrIguez M., Viegas R. M. C., Luque S., Coelhoso I. M., Crespo J. P. S. G., Alvareza J. R., Removal of Valeric Acid from Wastewaters by Membrane Contactors, *Journal of membrane science*, **137**: 45-53 (1997).

[26] Marinovic V., Ristic M., Dostanic M., Dynamic Adsorption of Trinitrotoluene on Granular Activated Carbon, *Journal of Hazardous Materials*, **117**: 121-128(2005).

[27] Zaitan H., Bianchi D., Achak O., Chafik T., A Comparative Study of the Adsorption and Desorption of O-Xylene onto Bentonite Clay and Alumina, *Journal of hazardous materials*, **153**: 852-859(2008).

[28] Pingdong W., Pigui Z., Adsorption of Low Molecular Weight Organic Acids on Polyvinylpyridine Resin, *Studies in Surface Science and Catalysis*, **80**: 729-735(1993).

[29] Mattson J., H. Mark, "Activated Carbon", Marcel Dekker, New York. (1971)

[30] Hadi M., Samarghandi M.R., McKay G., Simplified Fixed Bed Design Models for the Adsorption of Acid Dyes on Novel Pine Cone Derived Activated Carbon, *Water, Air, & Soil Pollution*, **218** 197-212 (2011).

[31] Kulkarni S., D.J. Kaware, Regeneration and Recovery in Adsorption-a Review‖, *International Journal of Innovative Science, Engineering & Technology*, **1**: 61-65 (2014).

[32] Bhaumik M., Setshedi K., Maity A., Chromium (VI) Removal from Water Using Fixed bed Column of Polypyrrole/Fe_3O_4 Nanocomposite, *Separation and Purification Technology*,110:11-19 (2013).

[33] Ji F., Li C., Xu J., Liu P. C., Dynamic Adsorption of Cu (II) From Aqueous Solution by Zeolite/Cellulose Acetate Blend Fiber in Fixed-Bed, *Colloids and Surface A: Physicochemical and Engineering Aspects*, **434**: 88-94 (2013).

[34] Pandey N.K., Velavendan P., Geetha R., Ahmed M.K., Koganti S.B., Adsorption Kinetics and Breakthrough Behaviour of Tri-n-butyl Phosphate on Amberlite XAD-4 Resin, *Journal of Nuclear Science and Technology*, 370-378 (1998).

[35] Lin S.H., Wang C.S., Chang C.H., Removal of Methyl tert-Butyl Ether from Contaminated Water by Macroreticular Resin, *Industrial & Engineering Chemistry Research*, **41**: 4116-4121 (2002).

[36] Han R., Zou L., Zhao X., Xu Y., Xu F., Li Y., Wang Y., Characterization and Properties of Iron Oxide-Coated Zeolite as Adsorbent for Removal of Copper (II) from Solution in Fixed Bed Column, *Chemical Engineering Journal*, **149**: 123–131 (2009).

[37] Maliyekkal S.M., Ligy Philip, Fixed-bed Adsorption of Arsenite (As(III)) from Drinking Water: *Breakthrough Studies and ModelingProceedings of the 3rd International CEMEPE & SECOTOX Conference Skiathos* (2011).

[38] Podder M., Majumder C., Fixed-Bed Column Study for As (III) and As (V) Removal and Recovery by Bacterial Cells Immobilized on Sawdust/$MnFe_2O_4$ Composite, *Biochemical Engineering Journal*, **105**: 114-135 (2016).

[39] Setshedi K. Z., Bhaumik M., Onyango M. S., Maityad A., Breakthrough studies for Cr (VI) sorption from Aqueous Solution Using Exfoliated Polypyrrole-Organically Modified Montmorillonite Clay Nanocomposite, *Journal of Industrial and Engineering Chemistry*, **20**: 2208-2216 (2014).

[40] Namane A., Hellal A., The Dynamic Adsorption Characteristics of Phenol by Granular Activated Carbon, *Journal of Hazardous Materials*, **137**: 618-625 (2006).

[41] McCabe W.L., Smith J.C., Harriott P., Unit Operation of Chemical Engineering, McGraw-Hill, New York, USA (1993).

[42] Hadi M., Samarghandi M.R, McKay G., Simplified Fixed Bed Design Models for the Adsorption of Acid Dyes on Novel Pine Cone Derived Activated Carbon, *Water, Air, & Soil Pollution*, **218**: 197-212 (2011).

[43] Albadarin A. B., Mangwandi C., Al-Muhtaseb A., Walker G. M., Allen S. J., Ahmad M. N., Modelling And Fixed Bed Column Adsorption of Cr(VI) onto Orthophosphoric Acid-Activated Lignin, *Chinese Journal of Chemical Engineering*, **20**: 469-477(2012).

[44] Owen D.M., Removal of DBP Precursors by GAC Adsorption, American Water Works Association (1998).

[45] Mohammed S.A., Faisal ., Alwan M.M, Oily Wastewater Treatment Using Expanded Beds of Activated Carbon and Zeolite, *Iraqi Journal of Chemical and Petroleum Engineering*,12 (2011)

[46] JG H., EK H., Energy Footprint and Operating Costs, A Comparison of Ion Exchange Resin and Activated Carbon in the Application of Sugar Decolourisation, *Proc. S Afr. Sug. Technol. Ass.*: 469-473(2017).

[47] Reimerink W., The Use of Activated Carbon as Catalyst and Catalyst Carrier in Industrial Applications, *Study in Surface Science and Catalysis*: 751-769(1999).

[48] Kuiper A., Medema J., Van Bokhoven J., Infrared And Raman Spectra of Benzaldehyde Adsorbed on Alumina, *Journal of Catalysis*, **29**: 40-48 (1973).

[49] Al Lafi A.G., Al Abdullah J., Cesium and Cobalt Adsorption on Synthetic Nano Manganese Oxide: A Two Dimensional Infra-Red Correlation Spectroscopic Investigation, *Journal of Molecular Structure*, **1093**: 13-23(2015).

[50] Sun W., Liu W., Hu Y., FTIR Analysis of Adsorption of Poly Diallyl-Dimethyl-Ammonium Chloride on Kaolinite, *Journal of Central South University of Technology*,**15**: 373-377(2008).

[51] Saraji S., Goual L., Piri M., Dynamic Adsorption of Asphaltenes on Quartz and Calcite Packs in the Presence of Brine Films, Colloids and Surfaces A: *Physicochemical and Engineering Aspects*, **434**: 260-267(2013).

[52] Dąbrowski A., Adsorption- from Theory to Practice, *Advanced in Colloid and Interface Science*, **93**: 135-224 (2001).

[53] Nekoo S.H., Fatemi S., Experimental Study and Adsorption Modeling of COD Reduction by Activated Carbon For Wastewater Treatment of Oil Refinery, *Iran. J. Chem. Chem. Eng. (IJCCE)*, **32**: 81-89(2013).

[54] Han R., et al., Characterization And Properties Of Iron Oxide-Coated Zeolite as Adsorbent for Removal of Copper (II) from Solution in Fixed Bed Column, *Chemical Engineering Journal*,**149**: 123-131(2009).

[55] Roque-Malherbe R.M., "Adsorption and Diffusion in Nanoporous Material", CRC Press Taylor & Francis Group, United Kingdom (2007).

[56] Coates J.,"Interpretation of Infrared Spectra, A Practical Approach John Coates Coates Consulting", Coates Consulting, Newtown, USA (2006).

[57] Han R., Wang Y., Yu W., Zou W., Shi J., Liu H., Biosorption of Methylene Blue from Aqueous Solution by Rice Husk in a Fixed-Bed Column, *Journal of Hazardous Materials*, **141**: 713-718 (2007).

[58] Futalan C., Kan C., Dalida M., Pascua C., Wan M., Fixed-Bed Column Studies on the Removal of Copper Using Chitosan Immobilized on Bentonite, *Carbohydrate Polymers*, **83**: 697-704(2011).

[59] Xu Z., Cai J.G., Pan B., Mathematically Modeling Fixed-Bed Adsorption in Aqueous Systems, *Journal of Zhejiang University Science A*, **14**: 155-176 (2013).

[60] Chu K.H., Fixed Bed Sorption: Setting the Record Straight on the Bohart–Adams and Thomas Models, *Journal of Hazardous Materials*, **177**: 1006-1012 (2010).

[61] Cabrera-Lafaurie W.A., Roman F.R., Hernández-Maldonado A.J., Single and Multi-Component Adsorption of Salicylic Acid, Clofibric Acid, Carbamazepine and Caffeine from Water onto Transition Metal Modified and Partially Calcined Inorganic–Organic Pillared Clay Fixed Beds, *Journal of Hazardous Materials*, **282**: 174-182(2015).